

Statistical Analysis of SiO₂ Contact Hole Etching in a Magnetically Enhanced Reactive Ion Etching Reactor

Chunli Liu^{1*} and B. Shrauner²

¹Department of Physics, Hankuk University of Foreign Studies, YongIn 449-791, Korea

²Department of Electrical and Systems Engineering, Washington University, St. Louis, MO 63130, USA

(Received 6 July 2010, Received in final form 27 August 2010, Accepted 31 August 2010)

Plasma etching of SiO₂ contact holes was statistically analyzed by a fractional factorial experimental design. The analysis revealed the dependence of the etch rate and DC self-bias voltage on the input factors of the magnetically enhanced reactive ion etching reactor, including gas pressure, magnetic field, and the gas flow rates of CHF₃, CF₄, and Ar. Empirical models of the DC self-bias voltage and etch rate were obtained. The DC self-bias voltage was found to be determined mainly by the operating pressure and the magnetic field, and the etch rate was related mainly to the pressure and the flow rates of Ar and CHF₃.

Keywords : Plasma, SiO₂, magnetically enhanced reactive ion etching

1. Introduction

Plasma etching of SiO₂ contact holes is a crucial step in integrated circuit fabrication [1, 2]. The feature shape defined in the etching process depends on many processing variables, such as the rf power, gas composition, reactor pressure, and gas flow rates. These variables often interact, which complicates process development. The dynamic characteristics and discharge parameters during the etching process have been numerically modeled [3-6]. In addition, the statistical study of plasma etching parameters through the technique of experimental design has recently been discussed because it can yield information about the effect of individual variables and the synergistic interaction between several parameters from experiential data [7-12]. The optimum etching conditions can be determined by applying a statistical model generated from multiple linear regressions of the independent variables affecting the etching process.

A linear regression model is generally used for the response and is represented in the following form [13]

$$Y = b_0 + b_1x_1 + b_2x_2 + \dots + b_kx_k + e, \quad (1)$$

where Y is the observable response, variables x_j ($j = 1, \dots, k$) are the functions of independent parameters (para-

meter only or interactions), and e is the statistical error. b_j ($j = 0, \dots, k$) are called regression coefficients and represent the expected change in response Y with per-unit change in x_j when all the remaining independent parameters x_i ($i \neq j$) are held constant. The regression coefficients are typically estimated by using the method of least squares [13].

The statistical investigation was applied to the etching process of various materials, including Si, GaAs, and SiO₂, in different etching systems [7, 8, 10, 11]. In most studies, a statistical technique was used to obtain a model for the response of interest, such as etch rate, etch uniformity, or anisotropy, which was then used to optimize the etching process within the process window. Kim and Kwon studied the etching of silica thin film by a full factorial experiment and noted the importance of the DC self-bias voltage in understanding the etching mechanism [11]. Riley *et al.* reported a study using a statistical model that succeeded in developing a uniform, selective SiO₂ sidewall spacer etching process in a Lam Research etching system [9].

Magnetically enhanced reactive ion etching (MERIE) is an important system configuration for plasma etching owing to its high etch rate at lower pressure. Research has focused on discharge models for plasma states and the effect of various magnetic field configurations during etching to optimize the etching process [3, 4, 14-16]. In addition to the discharge models, statistical models obtain-

*Corresponding author: Tel: +82-31-330-4733
Fax: +82-31-330-4566, e-mail: chunliliu@hufs.ac.kr

ed through experimental data have also provided an effective way to understand the dynamics of the etching process and to establish the optimum processing conditions. Buie and coworkers proposed a diagnostic method to identify the possible sources of reactive ion etching (RIE) lag and loading in a MERIE etching system through a statistical study [8]. In this paper, SiO₂ contact hole etching in a MERIE reactor was studied by using a 2⁵⁻¹ fractional factorial design, which is one type of experimental design [13]. Applied Materials (California, USA) supplied experimental data and scanning electron microscopy (SEM) images. The notation 2⁵⁻¹ means that the regression model has five parameters, each at two levels, represented by –1 and +1, respectively. In total, 2⁵⁻¹ = 16 runs are employed. The five independent parameters investigated in these experiments are the magnetic field (*B*), the total gas pressure in the chamber (*p*), the Ar gas flow rate (*Ar*), the CHF₃ gas flow rate (*CHF*₃), and the CF₄ gas flow rate (*CF*₄). The responses (*Y*) that we analyzed in this study include the DC self-bias voltage of the etching system, the etch rate of the contact holes, and the sidewall slope of the etch profile.

2. Experimental Setup

Etching of SiO₂ contact holes was conducted in a MERIE chamber for plasma etching of dielectrics manufactured by Applied Materials [17]. The chamber has four electromagnets controlled by two magnetic drives that allow two magnet pairs (a primary and a secondary pair) to be run at different magnetic field magnitudes [17, 18]. The stronger field in the primary pair was referred to as the magnetic field magnitude *B*. The magnetic field strength is as high as 100 G. The *B*-field ratio of the secondary pair to the primary was 0.2 in all the experiments in this work, so the secondary/primary ratio was not included in the experimental design.

Contact holes were etched through patterned boron phosphorous silicate glass (BPSG) about 2.0 μm thick on 200 mm Si wafers. Each thermal oxide wafer was etched

Table 1. Operation values of parameters.

Parameter	Value
<i>B</i>	5 or 35 G
<i>P</i>	100 or 300 mTorr
<i>CF</i> ₄	15 or 40 sccm
<i>CHF</i> ₃	45 or 70 sccm
<i>Ar</i>	100 or 200 sccm

for 200 s using a CHF₃, CF₄, and Ar gas mixture. The rf power was fixed at 1200 W. Helium at 20 Torr (~2.7 × 10³ Pa) was used for backside cooling. The operation values of the five parameters are shown in Table 1. The DC self-bias voltage was measured, and SEM images of etch profiles were taken at each point in the experimental design.

Etch profiles were obtained by using cross-sectional SEM looking perpendicularly at the edge of a centrally cleaved contact hole. Fig. 1 shows three typical SEM micrographs of SiO₂ contact hole etch profiles at the center of the patterned oxide. Several features of the profiles were observed in the SEM micrographs. The sidewall of the contact holes slanted slightly inward with a nearly constant slope. In some profiles, the slope of the bottom increased very slowly toward the sidewall, forming a microtrench at the corner of the bottom. The depth of the microtrench changed with the process conditions, and in some etches the bottom was flat.

3. DC Self-Bias Voltage Regression Model

The DC self-bias voltage is a measurement of the average ion energy impinging on the wafer surface; hence, it is important in process characterization and is useful in comparing plasma conditions between different systems. Using Eq. (1), we calculated the regression coefficients *b* of the five independent parameters and their interactions (multiplication of two independent parameters) for the response to the DC self-bias voltage bias. The values are shown in Table 2. The calculations were done in MATLAB. A comparison of the absolute values of the regression

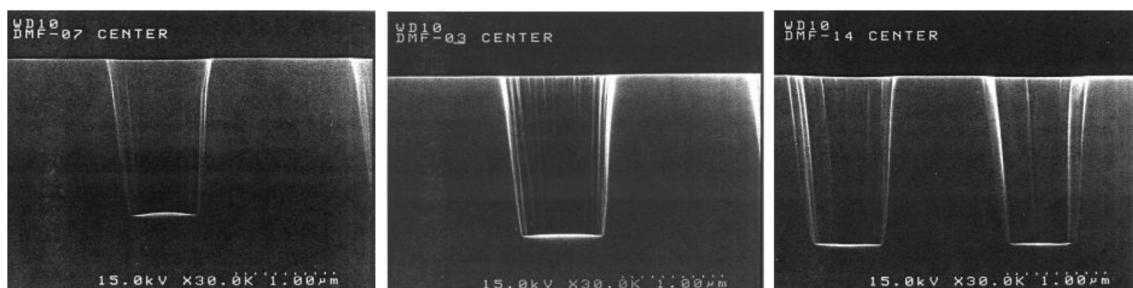


Fig. 1. SEM micrographs of SiO₂ contact hole etch profiles.

Table 2. Main effects of parameters and their interactions on DC bias voltage.

Parameter	<i>P</i>	<i>B</i>	<i>Ar</i>	<i>CHF₃</i>	<i>CF₄</i>
<i>b</i>	-64.9375	-59.0625	0.4375	-0.9375	0.0625
Interaction	<i>p</i> × <i>B</i>	<i>p</i> × <i>Ar</i>	<i>p</i> × <i>CHF₃</i>	<i>p</i> × <i>CF₄</i>	<i>B</i> × <i>Ar</i>
<i>b</i>	20.187	-1.3125	0.5625	-0.4375	-0.9375
Interaction	<i>B</i> × <i>CHF₃</i>	<i>B</i> × <i>CF₄</i>	<i>Ar</i> × <i>CHF₃</i>	<i>Ar</i> × <i>CF₄</i>	<i>CHF₃</i> × <i>CF₄</i>
<i>b</i>	0.4375	0.1875	0.4375	-0.3125	1.0625

coefficients for the listed factors shows that the contributions of the pressure (*p*) and magnetic field (*B*) and the interaction between these two parameters are much greater than those of all other terms. This indicates that these three terms were significant factors in determining the DC self-bias voltage of this etching system.

According to the results discussed above, the linear regression model for the DC self-bias voltage as a function of the pressure and magnetic field can be expressed as follows with the least-squares estimate of the regression coefficients:

$$V_{DC} = 387.5625 - 64.9375 p - 59.0625 B + 20.1875 (p \times B). \tag{2}$$

The variables *p* and *B* represent the pressure and the magnetic field, respectively, on a (-1, +1) scale, and *p*×*B* represents the level product of the pressure and the magnetic field. This regression model can be used to generate the predicted DC self-bias voltage across the range of designed process conditions. The negative coefficients for the pressure and magnetic field indicate that the DC self-bias voltage decreased as the pressure and magnetic field increased.

In Fig. 2, the diamond symbols represent the comparison between the predicted DC self-bias voltage (absolute

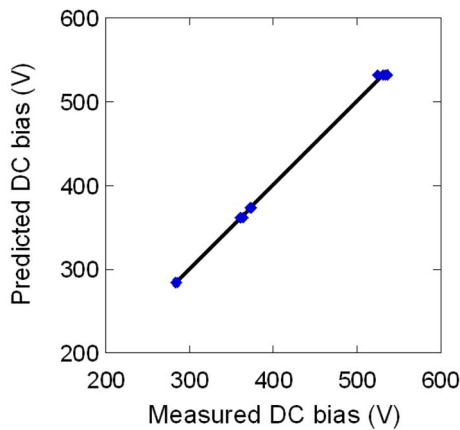


Fig. 2. Comparison of predicted DC self-bias voltage from the linear regression model and measured values.

values) under the process conditions of all 16 experiments and the experimentally measured DC self-bias voltages (absolute values). The straight line represents the diagonal axis on which the predicted value equals the measured value. The results showed an excellent fit between the predicted and measured DC self-bias voltages under most of the conditions in the 16 experiments. We concluded from this that the DC self-bias voltage bias in this etching system was very well defined by the magnetic field and the total gas pressure in the chamber. The suitability of a model can be measured by the *R*² index. The *R*² index of the DC self-bias voltage regression model was 99.93%.

The DC self-bias voltage is the DC potential across the sheath region, so it directly determines the ion flux and ion bombardment energy during etching. Therefore, it is one of the most important factors determining the etching characteristics [5, 19]. The effects of the magnetic field and pressure on the DC self-bias voltage bias identified in the above statistical analysis were consistent with the results reported in the literature. The primary effect of the magnetic field in the MERIE reactor was to increase the confinement of the electrons in the bulk plasma above the wafer, which in turn increased the ionization efficiency of neutral species, or the plasma density [6, 16, 20]. The DC self-bias voltage decreased with increasing magnetic field strength, while the ion densities in the CF₄ plasma increased [21]. Similar results for the magnetic field dependence of the DC self-bias voltage were also reported for magnetron sputtering deposition [22, 23]. The increase in plasma density in the glow discharge reduced the thickness of the ion sheath, so the sheath capacitance increased, and hence the self-bias voltage in the sheath region decreased.

The effect of pressure on the DC self-bias voltage can also be explained by the change in sheath thickness. Increasing pressure decreases electron diffusion toward the electrode because of an increase in electron-neutral collisions, so the DC self-bias voltage also decreases as the pressure increases [19]. The sheath thickness and DC self-bias voltage were found to decrease with increasing pressure at 53-400 mTorr [24] and 20-200 mTorr [25]. The measurements showed that the capacitive reactance of the sheath decreased at higher pressures. These studies also showed that the pressure dependence of the DC self-bias voltage was independent of the gas species. Camacho and Morgan reported the same observation in a study of GaAs via etching using Cl₂ and SiCl₄ gases in an RIE reactor [10]. The dependence of the DC self-bias voltage on the gas pressure and the magnetic field has been demonstrated separately, but the statistical analysis is a new result, as both factors act simultaneously and interact.

4. Etch Rate Regression Model

The etch rate of a SiO₂ contact hole was obtained by measuring the depth of the contact hole from its SEM micrograph and then dividing the depth by the etch time. The radius of each contact hole was about 1 μm. The regression coefficients of the five independent parameters and their interactions with respect to the etch rate were calculated and are shown in Table 3. The values of the regression coefficients for p , Ar , and the $p \times Ar$, $Ar \times CHF_3$, and $p \times CHF_3$ interactions were greater than those of the other terms in absolute magnitude. Therefore, we considered these effects to be important for predicting the etch rate of SiO₂ contact holes. The linear regression model of the etch rate is

$$ER = 7.9063 - 0.1625 p - 0.2937 Ar - 0.3875 (p \times Ar) + 0.3375 (Ar \times CHF_3) + 0.2188 (p \times CHF_3), \quad (3)$$

where ER is the etch rate in nm/s, and the variables p , Ar , and CHF_3 represent the pressure, Ar flow rate, and CHF_3 flow rate, respectively, on a (-1, +1) scale.

The etch rate analyzed here was the average net etch rate, *i.e.*, the difference between the etch rate and the deposition rate. The decrease in the net etch rate as the Ar flow rate increased can be explained by Ar gas dilution of the reactive species in the plasma. The etching of SiO₂ was a combined effect of surface ion bombardment and reactions between the etching gas and the SiO₂. Although increasing the Ar gas flow rate may increase the ion flux arriving at the surface, it may also reduce the availability of reactive species in the discharge, which in turn decreases the etch rate. Increasing the pressure can cause more collisions between neutral species and decrease the dissociation of gas molecules, decreasing the etch rate. The DC self-bias voltage also decreases as the pressure increases, as indicated by the DC self-bias voltage model, and this could be another reason for the decrease in the etch rate. The CHF_3 flow rate affects the etch rate through changes in the densities of CHF_2 radicals and CHF_2^+ ions, which have been reported to affect the deposition of polymer films [26].

Table 3. Main effects of parameters and their interactions on etch rate (all in nm/s).

Parameter	P	B	Ar	CHF ₃	CF ₄
b	-0.1625	0.0875	-0.2937	0.0375	0.1
Interaction	$p \times B$	$p \times Ar$	$p \times CHF_3$	$p \times CF_4$	$B \times Ar$
b	0.0063	-0.3875	0.2188	0.0313	0
Interaction	$B \times CHF_3$	$B \times CF_4$	$Ar \times CHF_3$	$Ar \times CF_4$	$CHF_3 \times CF_4$
b	0.0438	-0.0563	0.3375	-0.0875	0.1188

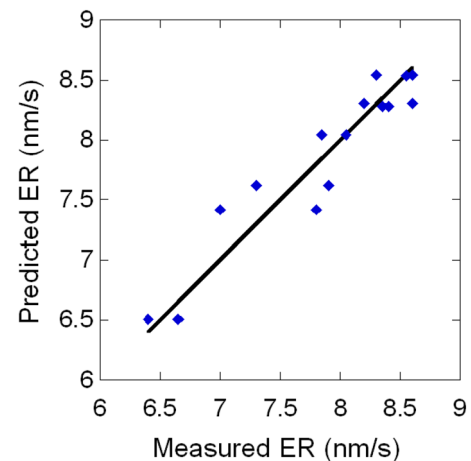


Fig. 3. Comparison of etch rates predicted from the linear regression model and measured values.

Fig. 3 compares the etch rates under the process conditions of all 16 experiments predicted from Eq. (3) and the etch rates measured from the SEM micrographs. The solid line in Fig. 3 follows the diagonal axis at which the predicted and measured values are equal. The diamonds represent the comparison results, showing that the predicted etch rates are close to the actual etch rates. By comparing the predicted DC self-bias voltage and etch rates, we can see that the etch rate prediction was not as good as that of the DC self-bias voltage. The reason is that the etch rate is affected by almost every factor in the etching process, and the mechanism is very complicated. In this experiment, the etch rate was determined mainly by the pressure, the Ar flow rate, and the two-factor interactions between the pressure, Ar flow rate, and CHF_3 flow rate. Other factors also affect the etch rate, but the effects were relatively small. The R^2 index of the etch rate regression model was 91%.

5. Etch Profile Investigation

In addition to the DC self-bias voltage and the etch rate of the contact holes, it is important to determine the optimum process conditions for the etch profile. The ideal etch profile of a contact hole should have a slightly slanted sidewall with a flat bottom and rounded corners, so that the device area can be minimized and the contact hole can be filled in the next processing step without forming voids in the corners. Voids could increase the thermal stresses on the underlying silicon and degrade device function.

We chose the sidewall slope of the etch profile as a response variable. The sidewall slope was defined as the angle between the sidewall of the etch profile and the

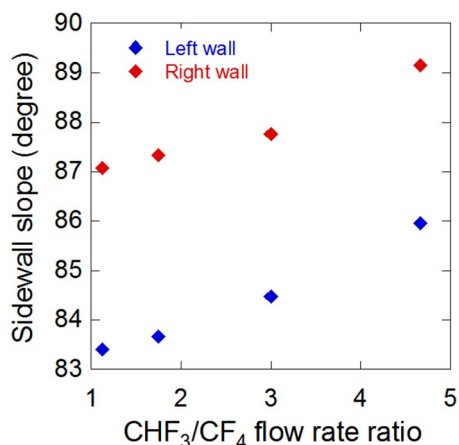


Fig. 4. Changes in sidewall slope with CHF₃/CF₄ ratio.

horizontal direction. The sidewall slopes of SiO₂ contact holes were measured from SEM micrographs. Regression coefficients for individual parameters and their interactions were first calculated as described for the DC self-bias voltage model and the etch rate model, but in this case the statistical analysis provided no indications about which effect was significant with respect to the sidewall slope. However, we observed from the SEM micrographs that the sidewall slope of the contact hole changed significantly with the CHF₃/CF₄ ratio in the gas mixture. From the experimental design, we knew that there were two levels for the CHF₃ and CF₄ flow rates, so there were four combinations of CHF₃/CF₄ ratios in the etching conditions, *i.e.*, 45/40, 45/15, 70/40, and 70/15. Fig. 4 illustrates the change in right-sidewall slopes with CHF₃/CF₄ ratio, where each point represents the average of the etch profile slopes under the same CHF₃/CF₄ ratio.

Fig. 4 shows that the sidewall slope increased as the CHF₃/CF₄ ratio increased. That is, the sidewall of the contact hole was more steeply sloped (more vertical) when the gas mixture contained more CHF₃. Although the slope of the left sidewall was about 3° less than that of the right sidewall owing to asymmetry in the etch profile, both sidewall slopes show the same trend with respect to the CHF₃/CF₄ ratio. Similar experimental results have been reported for SiO₂ contact hole etching [26]. One explanation is the effect of the CHF₃/CF₄ ratio on the sidewall polymer deposition rate. In RIE of SiO₂ wave guides with CHF₃/CF₄/Ar gas, the polymer deposition rate in the area shielded from ion bombardment was found to decrease with increasing CHF₃/CF₄ ratio in the plasma [11, 26]. In fluorocarbon plasmas, with an increase in the H₂ addition in the plasma, which was similar to the addition of CHF₃, the etch rate of SiO₂ increased first and then decreased or became zero [27]. The thickness of the

polymer was closely related to the oxide etch rate. In the process conditions we studied, the etching could be in a state such that an increase in CHF₃ mainly increased the oxide etch rate, or the surface reaction rate between the polymer and the SiO₂ was fast enough to suppress the accumulation of polymer on the etch surface. Therefore, the sidewall slope increased with the CHF₃/CF₄ ratio.

6. Conclusions

Experimental data from a 2⁵⁻¹ fractional factorial experimental design were analyzed for the effects of pressure, magnetic field, and gas flow rates of Ar, CHF₃, and CF₄ on the DC self-bias voltage and plasma etching characteristics, including the etch rate and etch profiles, of SiO₂ contact holes. Linear regression models for the DC bias and the etch rate were developed from the collected data. The DC self-bias voltage was found to be determined mainly by the operating pressure and the magnetic field. The etch rate was related mainly to the pressure and the flow rates of Ar and CHF₃. The sidewall slope of the contact hole increased with increasing CHF₃/CF₄ flow rate ratio, indicating that the etching process can be preliminarily estimated on the basis of the CHF₃/CF₄ ratio. The empirical models quite accurately represent the behavior of a MERIE reactor under a certain range of etch recipes, which may be readily extended to other SiO₂ etching processes with similar equipment and gas mixtures and used to optimize the etching process.

Acknowledgements

This work was supported by the Hankuk University of Foreign Studies research fund of 2010. The authors thank M. Buie and J. Pender in Applied Materials for supplying the SEM images and experimental data.

References

- [1] B. Wu, *J. Vac. Sci. Technol. B* **24**, 1 (2006).
- [2] B. Jinnai, T. Orita, M. Konishi *et al.* *J. Vac. Sci. Technol. B* **25**, 1808 (2007).
- [3] M. A. Lieberman, A. J. Lichtenberg, and S. E. Savas, *IEEE Trans. Plasma Sci.* **19**, 189 (1991).
- [4] J. C. Park and B. K. Kang, *IEEE Trans. Plasma Sci.* **25**, 499 (1997).
- [5] S. J. You, S. K. Ahn, and H. Y. Chang, *Surf. Coat. Tech.* **193**, 81 (2005).
- [6] S. H. Lee, S. J. You, H. Y. Chang, and J. K. Lee, *J. Vac. Sci. Technol. A* **25**, 455 (2007).
- [7] G. S. May, J. Huang, and C. J. Spanos, *IEEE Trans. Semicond. Manuf.* **4**, 83 (1991).

- [8] M. J. Buie, J. T. Pender, and P. L. G. Ventzek, *Jpn. J. Appl. Phys. Part 1* **36**, 4838 (1997).
- [9] P. E. Riley, V. D. Kulkarni, and S. H. Bishop, *J. Vac. Sci. Technol. B* **7**, 24 (1989).
- [10] A. Camacho and D. V. Morgan, *J. Vac. Sci. Technol. B* **12**, 2933 (1994).
- [11] B. Kim and K. H. Kwon, *J. Appl. Phys.* **93**, 76 (2003).
- [12] W. Guo and H. H. Sawin, *J. Phys. D-Appl. Phys.* **42**, 194014 (2009).
- [13] G. E. P. Box, W. G. Hunter, and J. S. Hunter, *Statistics for Experimenters: An Introduction to Design, Data Analysis, and Model Building*, John Wiley & Sons, New York (1978).
- [14] S. Nakagawa, T. Sasaki, H. Mori, and T. Namura, *Jpn. J. Appl. Phys. Part 1* **33**, 2194 (1994).
- [15] H. C. Shin, K. Noguchi, X. Y. Qian, N. Jha, G. Hills, and C. Hu, *IEEE Electron Device Lett.* **14**, 88 (1993).
- [16] Y. Li, A. Iizuka, and N. Sato, *Phys. Rev. B* **132**, 585 (1997).
- [17] M. J. Buie, J. T. P. Pender, and M. Dahimene, *J. Vac. Sci. Technol. A* **16**, 1464. (1998).
- [18] R. Lindley, C. Bjorkman, H. Shan *et al.* *Solid State Technol.* **40**, 93 (1997).
- [19] S. J. You, C. W. Chung, K. H. Bai, and H. Y. Chang, *Appl. Phys. Lett.* **81**, 2529 (2002).
- [20] M. A. Lieberman and A. Lichtenberg, *Principles of Plasma Discharges and Materials Processing*, John Wiley & Sons, New York (1994).
- [21] G. Y. Yeom and M. Kushner, *Appl. Phys. Lett.* **56**, 857 (1990).
- [22] A. Furuya and S. Hirono, *J. Appl. Phys.* **68**, 304 (1990).
- [23] A. Furuya and S. Hirono, *J. Appl. Phys.* **87**, 939 (2000).
- [24] A. J. Van Roosmalen, W. G. M. Van den Hoek, and H. Kalter, *J. Appl. Phys.* **58**, 653 (1985).
- [25] A. Seabaugh, *J. Vac. Sci. Technol. B* **6**, 77 (1988).
- [26] M. V. Bazylenko and M. Gross, *J. Vac. Sci. Technol. A* **14**, 2994 (1996).
- [27] D. L. Flamm, in *Plasma Etching, An Introduction*, edited by D. M. Manos and D. L. Flamm, Academic Press, Boston (1989).